Quantum fluctuations in a strongly interacting Bardeen-Cooper-Schrieffer polariton condensate at thermal equilibrium

Hui Hu and Xia-Ji Liu

Centre for Quantum and Optical Science, Swinburne University of Technology, Melbourne, Victoria 3122, Australia

Microcavity electron-hole-photon systems in two dimensions have long been anticipated to exhibit a crossover from Bose-Einstein condensate (BEC) to Bardeen-Cooper-Schrieffer (BCS) superfluid when the carrier density is tuned to reach the Mott transition density. Yet, a theoretical understanding of such a BEC-BCS crossover largely relies on the mean-field framework and the nature of the carriers at the crossover remains unclear to some extent. Here, motivated by the recent demonstration of a BCS polariton laser [arXiv:1902.00142] and based on a simplified short-range description of the electron-hole attraction, we examine the role of quantum fluctuations in an exciton-polariton condensate at thermal equilibrium and determine the number of different types of carriers at the crossover beyond mean field. Near Mott density and with very strong light-matter coupling, we find an unexpectedly large phase window for a strongly correlated BCS polariton condensate, where both fermionic Bogoliubov quasiparticles and bosonic excitons are significantly populated and strongly couple to photons. We predict its absorption spectrum and show that the upper polariton energy gets notably renormalized, giving rise to a high-energy side-peak at large carrier density, as observed in recent experiments.

Over the past two decades, the realization of quantum fluids of electron-hole-photon condensates in semiconductor microcavities [1–4] has opened a new era for better photonic technologies [5,6]. In most situations with low carrier density, tightly bound electron-hole (*e-h*) pairs can be well approximated as structureless point-like bosons of small Bohr radius a_B. Coupled with photons, they turn into quasiparticles (i.e., exciton-polaritons) and undergo Bose-Einstein condensation (BEC) at sufficiently low temperatures [1–4]. When carrier density is high, comparable to a characteristic Mott transition density $n_{\text{mott}} \sim a_B^{-2}$, the composite nature of *e-h* pairs becomes important and the emerging fermionic degree of freedoms may eventually lead to a Bardeen-Cooper-Schrieffer (BCS) polariton condensate [7], where the loosely bound fermionic *e-h* pairs are formed by photon-mediated attractions [8–10], rather than Coulomb interactions that turn out to be screened. This high-density regime was recently investigated in several experiments [11–13]. While the strong coupling between *e-h* pairs and photons was confirmed via the observation of a negative excitation branch [12] and a puzzling high-energy side peak [11] in photoluminescence, the existence of a BCS polariton condensate remains elusive. In the highly nonequilibrium lasing regime, the signature of a BCS polariton laser was recently demonstrated [14].

Microscopic theoretical description of the evolution from an exciton-polariton BEC to a BCS polariton condensate, the so-called BEC-BCS crossover, is highly nontrivial for several reasons: (i) The interparticle Coulomb interactions are strong and long range; (ii) the coupling between light and matter can also be nonperturbative in the *verystrong* coupling regime achieved so far in experiment [15,16], where the characteristic Rabi coupling Ω can be comparable to the binding energy E_B of excitons; (iii) electron-hole-photon systems are often

confined in a single-layer quantum well and therefore are two dimensional in character, where both quantum and thermal fluctuations are significant [17]; and (iv) the systems are inherently nonequilibrium. Continuous pumping is necessary to compensate the loss in carriers in order to keep a steady state [1,2]. The first theoretical study of the challenging problem of BEC-BCS crossover with exciton-polaritons was provided by Littlewood and coworkers [18–20] by treating localized excitons as a collection of two-level systems. A more formal treatment was later developed by Kamide *et al.* [21] and Byrnes *et al.* [22] by using the celebrated BCS variational wave functions. While the mean-field BCS wave function permits a description of fermionic quasiparticles and of condensed photons and gives a useful equilibrium phase diagram [21,23], strictly speaking, it does not provide information on the key ingredient of exciton-polariton quasiparticles, which should be obtained by taking into account quantum fluctuations beyond mean field. More seriously, in the limit of strong coupling, the mean-field framework may simply break down in two dimensions, even at the qualitative level, as shown by the recent investigation of the BEC-BCS crossover in a two-dimensional strongly interacting Fermi gas [24,25].

The purpose of this Rapid Communication is to deepen our understanding of polariton quasiparticles in strongly interacting BCS polariton condensates, by adopting a zero-temperature Gaussian pair fluctuation (GPF) theory [25–29]. A qualitatively different, more reliable phase diagram at thermal equilibrium is then determined (see Fig. 1). The inclusion of the crucial quantum fluctuations comes at a price. We need to replace the long-range Coulomb force between electrons and holes by a *short-range* contact interaction. This seems to be a reasonable approximation in the dilute exciton limit, where the strength of the contact interaction is tuned to
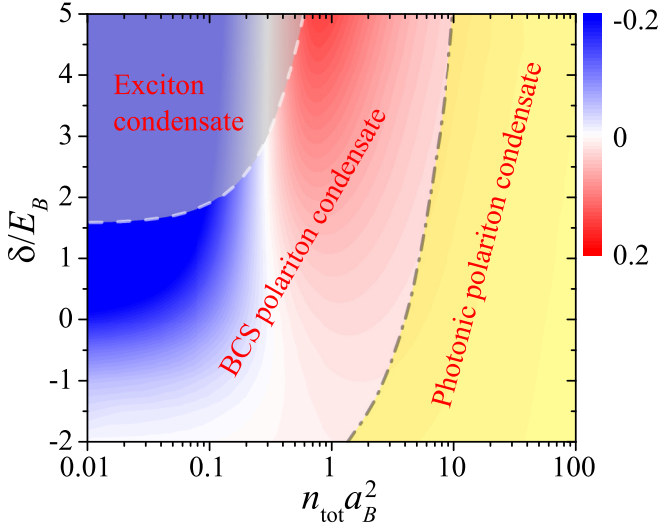
FIG. 1. Zero-temperature phase diagram as functions of the total carrier density n_{tot} (in units of $n_{\text{mott}} = a_B^{-2}$) and the cavity detuning δ (in units of E_B), at the light-matter coupling $\Omega = 0.8E_B$. The color shows the difference in density fractions of fermionic quasiparticles and excitons. The phase diagram is divided into three parts by the dashed and dot-dashed lines, which indicate 10% and 90% photonic fractions, respectively. A BCS polariton condensate forms in between, where Bogoliubov quasiparticles and excitons coexist. The boundaries between different phases should be understood as crossover, rather than phase transition.

reproduce the exact binding energy of excitons. Towards the high-density regime, the approximation may get improved, considering the gradual screen of Coulomb interactions and the increasingly dominant role played by the light-matter coupling. We note that a contact electron-hole interaction was previously used in the mean-field treatment, which leads to more or less similar results as the long-range Coulomb interaction [30]. In this work we also consider the equilibrium situation only, as inspired by the recent experimental demonstration of a *thermal* equilibrium exciton-polariton BEC in a high-quality microcavity [31]. The extension of our work to include dissipations is possible, following the standard Keldysh technique [32–34].

Our key results can be briefly summarized as follows: First, as shown in Fig. 1, in the very strong-coupling regime we observe an unexpectedly wide phase space for BCS polariton condensate with strongly correlated *e-h* pairs coupled to photons. The window for conventional exciton-polariton BEC shrinks due to very strong light-matter coupling. A BCS superfluid of *e-h* pairs only, anticipated in the previous studies [21], is also not favorable. Second, at high carrier density where photons become dominant, the system remains strongly coupled or correlated, as indicated by a large fraction of noncondensed photons. It is then better characterized as a photonic polariton condensate. This picture is consistent with earlier theoretical [35] and experimental investigations [11,12]. Finally, with increasing carrier density, we find that both lower and upper polariton energies of the BCS polariton condensate get strongly renormalized. In particular, the upper polariton branch shifts up significantly. This finding may

provide a qualitative explanation for the puzzling observation of a high-energy side-peak in emission spectra at high densities [11].

Microcavity electron-hole-photon systems. We start by considering the following approximate model Hamiltonian in two dimensions with area $\mathcal{S} = 1$ [26,30,34]:

$$\mathcal{H} = \sum_{\mathbf{k}\sigma} \xi_{\mathbf{k}} c_{\mathbf{k}\sigma}^{\dagger} c_{\mathbf{k}\sigma} + u_0 \sum_{\mathbf{kk'q}} c_{\frac{\mathbf{q}}{2}+\mathbf{k}e}^{\dagger} c_{\frac{\mathbf{q}}{2}-\mathbf{k}h}^{\dagger} c_{\frac{\mathbf{q}}{2}-\mathbf{k'}h} c_{\frac{\mathbf{q}}{2}+\mathbf{k'}e}$$
$$+ g_0 \sum_{\mathbf{kq}} \left(\phi_{\mathbf{q}}^{\dagger} c_{\frac{\mathbf{q}}{2}-\mathbf{k}h} c_{\frac{\mathbf{q}}{2}+\mathbf{k}e} + \text{H.c.} \right) + \sum_{\mathbf{q}} \omega_{\mathbf{q}} \phi_{\mathbf{q}}^{\dagger} \phi_{\mathbf{q}}, \quad (1)$$

where $c_{\mathbf{k}\sigma}$ are the annihilation operators of electrons ($\sigma = e$) and holes ($\sigma = h$) with dispersion $\xi_{\mathbf{k}} \equiv \hbar^2 \mathbf{k}^2/(2m_{\text{eh}}) - \mu_{\text{eh}}/2$, and $\phi_{\mathbf{q}}$ are the annihilation operators of photons with dispersion $\omega_{\mathbf{q}} \equiv \hbar^2 \mathbf{q}^2/(2m_{\text{ph}}) + \delta_0 - \mu_{\text{ph}}$. In both dispersion relations, the chemical potentials (μ_{eh} for electrons or holes and μ_{ph} for photons) are measured from the band gap E_g of the semiconductor quantum well and are the same in equilibrium. For convenience, we have assumed the same mass $m_{\text{eh}} \simeq 0.068m_0$ for electrons and holes (where m_0 is the mass of free electrons) [1,34]. The mass of photons due to quantum well confinement is instead much smaller and we set $m_{\text{ph}} \simeq 3 \times 10^{-5} m_0$ [1,34]. The detuning of the microcavity with respect to the band edge is denoted by δ_0 and is to be replaced with $\delta = E_{\text{cav}} - E_g$ upon renormalization [36]. The second and third terms in the Hamiltonian describe the electron-hole attraction and light-matter coupling, respectively, with *bare* interaction strengths (u_0 and g_0), which are to be renormalized to reproduce the observable exciton binding energy E_B and Rabi coupling Ω. We refer to Supplemental Material [36] for two-body physics and the detailed procedure of renormalization. From now on, we always use the renormalized parameters u, g, and δ in equations.

The Hamiltonian (1) provides a reasonable *minimal* model of electron-hole-photon systems in microcavity [30,34]. As the light-matter coupling generates an effective attraction between electrons and holes [8–10], which eventually dominates over the direct Coulomb interaction at high carrier density, we anticipate that the replacement of Coulomb interaction in terms of a short-range contact interaction only brings corrections at the *quantitative* level. We note that the model Hamiltonian also describes a strongly interacting Fermi gas of ultracold atoms near a narrow Feshbach resonance [26], which unfortunately suffers from severe atom loss [37]. A near-equilibrium high-density exciton-polariton therefore realizes an interesting example to explore the many-body physics with large effective range of interactions [37–39].

Gaussian pair fluctuation framework. The use of a short-range electron-hole attraction allows us to understand the crucial role of quantum fluctuations in exciton-polariton condensates within the reliable GPF theory [25–29,40]. It can be mostly easily derived with the help of the functional path-integral approach, as given in the Supplemental Material [36]. Here, we briefly review the key steps. By using the Hubbard–Stratonovich transformation, we first introduce a pairing field to decouple the electron-hole interaction term and integrate out the fermionic fields $c_{\mathbf{k}\sigma}$. This leads to an effective action for the pairing field and photon field. The saddle-point solution of both fields (more precisely, their superposition)

then gives rise to the mean-field thermodynamic potential at $T = 0$ [36],

$$\Omega_{\mathrm{MF}} = -\frac{\Delta^2}{u_{\mathrm{eff}}} + \sum_{\mathbf{k}} \left[\xi_{\mathbf{k}} - E_{\mathbf{k}} + \frac{\Delta^2}{\hbar^2 \mathbf{k}^2/m_{\mathrm{eh}} + \varepsilon_0} \right], \quad (2)$$

where Δ is an order parameter to be determined by the gap equation $\partial\Omega_{\mathrm{MF}}/\partial\Delta = 0$, $u_{\mathrm{eff}} \equiv u + g^2/(\mu_{\mathrm{ph}} - \delta)$ is an effective interaction incorporating the photon-mediated attraction [8,10], $E_{\mathbf{k}} \equiv (\xi_{\mathbf{k}}^2 + \Delta^2)^{1/2}$ is the dispersion relation for fermionic quasiparticles, and $\varepsilon_0 \ll E_B$ is an unimportant energy scale to regularize the logarithmic infrared divergence in two dimensions [36]. According to the standard BCS theory, the mean-field thermodynamic potential in Eq. (2) describes the *fermionic* Bogoliubov quasiparticles, as well as the *condensed* photons. To go beyond mean field, we consider the bilinear Gaussian fluctuations around the saddle point, which may physically be interpreted as *polaritons*. Integrating out these fluctuations, we obtain the GPF thermodynamic potential from quantum fluctuations [36],

$$\Omega_{\mathrm{GPF}} = \frac{1}{2} k_B T \sum_{\mathcal{Q}} \ln\left[M_{11} M_{22} - M_{12} M_{21} \right] e^{i\nu_n 0^+}, \quad (3)$$

where $\mathcal{Q} \equiv (\mathbf{q}, i\nu_n)$ with bosonic Matsubara frequencies $\nu_n = 2\pi n k_B T$ ($n \in \mathbb{Z}$) and $M_{ij}(\mathcal{Q})$ ($i, j = 1, 2$) are the matrix elements of the two by two polariton Green's function,

$$M_{11}(\mathcal{Q}) = M_{22}(-\mathcal{Q}) = \left[-\frac{1}{u_{\mathrm{eff}}(\mathcal{Q})} + \frac{1}{u_{\mathrm{eff}}} \right]$$
$$+ \sum_{\mathbf{k}} \left[\frac{u_+^2 u_-^2}{i\nu_n - E_+ - E_-} - \frac{v_+^2 v_-^2}{i\nu_n + E_+ + E_-} + \frac{1}{2E_{\mathbf{k}}} \right], \quad (4)$$

$$M_{12}(\mathcal{Q}) = M_{21}(+\mathcal{Q}) = \sum_{\mathbf{k}} u_+ v_+ u_- v_-$$
$$\times \left[\frac{1}{i\nu_n - E_+ - E_-} - \frac{1}{i\nu_n + E_+ + E_-} \right]. \quad (5)$$

Here, we define the short-hand notations, $E_{\pm} \equiv E_{\mathbf{k}\pm\mathbf{q}/2}$, $u_{\pm}^2 = (1 + \xi_{\mathbf{k}\pm\mathbf{q}/2}/E_{\mathbf{k}\pm\mathbf{q}/2})/2$, $v_{\pm}^2 = 1 - u_{\pm}^2$, and a momentum- and frequency-dependent effective interaction strength $u_{\mathrm{eff}}(\mathcal{Q}) \equiv u + g^2/[i\nu_n - \hbar^2 \mathbf{q}^2/(2m_{\mathrm{ph}}) + \mu_{\mathrm{ph}} - \delta]$. For a given $\mu_{\mathrm{eh}} = \mu_{\mathrm{ph}} = \mu$, we calculate the total thermodynamic potential $\Omega_{\mathrm{tot}} = \Omega_{\mathrm{MF}} + \Omega_{\mathrm{GPF}}$ and then determine the total density of carriers, $n_{\mathrm{tot}} = -\partial\Omega_{\mathrm{tot}}/\partial\mu$.

Nature of carriers and phase diagrams. According to the structure of mean-field and GPF thermodynamic potentials, $\Omega_{\mathrm{MF}}(\mu_{\mathrm{eh}}, \mu_{\mathrm{ph}})$ and $\Omega_{\mathrm{GPF}}(\mu_{\mathrm{eh}}, \mu_{\mathrm{ph}})$, we may distinguish *four* types of carriers:

$$n_{\mathrm{eh}} = -\frac{\partial\Omega_{\mathrm{MF}}}{\partial\mu_{\mathrm{eh}}} = \frac{1}{2} \sum_{\mathbf{k}} \left(1 - \frac{\xi_{\mathbf{k}}}{E_{\mathbf{k}}} \right), \quad (6)$$

$$n_{\mathrm{ph},0} = -\frac{\partial\Omega_{\mathrm{MF}}}{\partial\mu_{\mathrm{ph}}} = \left(\frac{g}{\delta - \mu_{\mathrm{ph}}} \right)^2 \frac{\Delta^2}{u_{\mathrm{eff}}^2}, \quad (7)$$

$n_{\mathrm{pl\text{-}ex}} = -\partial\Omega_{\mathrm{GPF}}/\partial\mu_{\mathrm{eh}}$, and $n_{\mathrm{pl\text{-}ph}} = -\partial\Omega_{\mathrm{GPF}}/\partial\mu_{\mathrm{ph}}$. The former two are the fermionic quasiparticles [41] and condensed photons, while the latter two could be understood as the
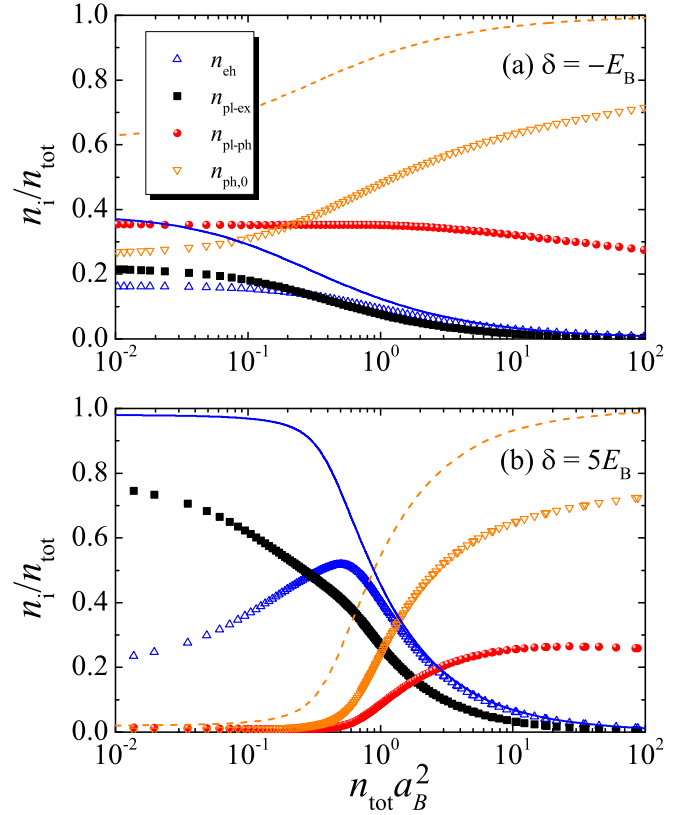

FIG. 2. Density fraction of different carriers as a function of the total carrier density (in units of a_B^{-2}), at the Rabi coupling $\Omega = 0.8E_B$ and the detuning (a) $\delta = -E_B$ and (b) $\delta = 5E_B$. For comparison, we also show the mean-field results for fermionic quasiparticles n_{eh} and condensed photons $n_{\mathrm{ph},0}$ using blue solid lines and orange dashed lines, respectively.

excitonic and photonic parts of the exciton-polariton quasiparticles [36]. In the previous studies [21,22,30], only the numbers of fermionic quasiparticles and condensed photons are accessible using a BCS variational wave function.

In Fig. 2, we show the density fraction of different carriers at zero cavity detuning [Fig. 2(a)] and at a large detuning [Fig. 2(b)] in different symbols, as a function of the total carrier density at a very strong light-matter coupling $\Omega = 0.8E_B$. To compare with earlier results [30], we plot also the mean-field prediction for n_{eh} and $n_{\mathrm{ph},0}$ with the solid and dashed lines, respectively. At zero detuning in Fig. 2(a), the photon energy E_{cav} is equal to the exciton energy $E_X = -E_B$; both of them are measured from the band-gap energy E_{g}. In the limit of low carrier density, in sharp contrast with the conventional exciton-polariton picture (i.e., a polariton consists of half exciton and half photon), we find that all the four carriers are notably populated, suggesting the appearance of a BCS-like polariton condensate, where the fermionic degree of freedom is important and $n_{\mathrm{eh}} \simeq n_{\mathrm{pl\text{-}ex}}$. The significant population of fermionic quasiparticles n_{eh} can be understood from the very strong light-matter coupling: As a result of $\Omega \sim E_B$, the internal fermionic degree of freedom of excitons is no longer frozen and can directly manifest itself in the few-body wave function, as discussed in a recent microscopic calculation [42]. The low-density situation at
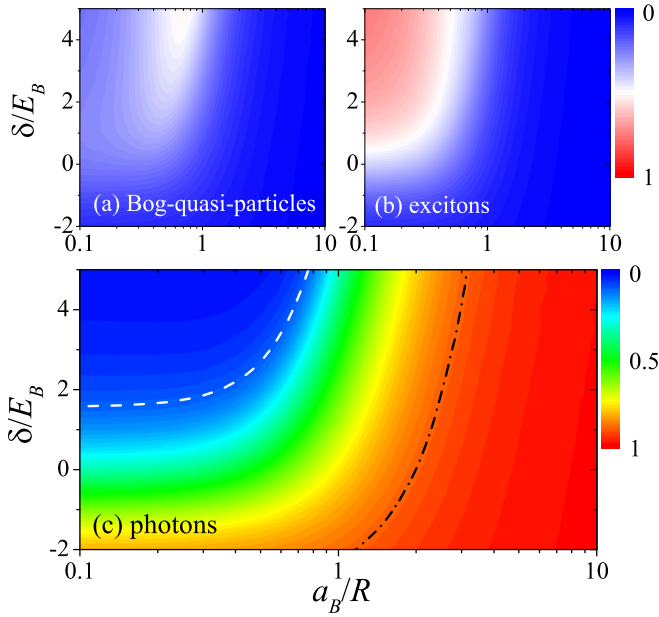
FIG. 3. Contour plot of the density fractions of fermionic (a) Bogoliubov quasiparticles, (b) excitons, and (c) photons as functions of the inverse mean particle distance $1/R = n_{\text{tot}}^{1/2}$ (in units of a_B^{-1}) and the detuning δ (in units of E_B). The dashed and dot-dashed lines in panel (c) show 10% and 90% photonic fractions, respectively.

a large cavity detuning in Fig. 2(b) seems to be different. Although n_{eh} is still non-negligible, photons are now depleted due to their large energy up-shift. The density of excitons, $n_{\text{pl-ex}}$, is dominant, much larger than n_{eh}. The system is then better viewed as an exciton condensate without photons. This picture becomes less accurate when the total carrier density increases, since the photon-mediated attraction plays an increasingly important role and drives the system into the BEC-BCS crossover regime with a notable photon fraction [26]. As a consequence, close to the Mott transition density $n_{\text{tot}} \sim a_B^{-2}$, we find again $n_{\text{eh}} \sim n_{\text{pl-ex}}$ and hence a strongly interacting BCS polariton condensate. Finally, at sufficiently large carrier density $n_{\text{tot}} \gg a_B^{-2}$, photons with density $n_{\text{ph}} = n_{\text{ph,0}} + n_{\text{pl-ph}}$ becomes dominant at both zero and large detunings due to the Bose enhancement [30] and forms a photonic condensate. This observation is consistent with earlier mean-field predictions [21,22,30]. However, our beyond-mean-field theory is able to reveal an important feature: Not all the photons are in the condensate and the density of *noncondensed* photons (i.e., $n_{\text{pl-ph}}$) is always significant as a result of the induced interaction mediated by residual matter [36]. To characterize this strong-coupling state, the system could be better termed as a photonic polariton condensate.

We now examine the detuning dependence of the different carrier fractions, as presented in the contour plot Figs. 3(a)–3(c) for fermionic quasiparticles n_{eh}, excitonic part of polaritons $n_{\text{pl-ex}}$, and total photons n_{ph}, respectively. Here, the dimensionless ratio $R = n_{\text{tot}}^{-1/2}/a_B$ measures the average distance between carriers relative to the Bohr radius of excitons. From Fig. 3(c), we can see clearly that the total photon density increases monotonically with decreasing cavity detuning δ or mean carrier separation R. The photon-rare and photon-rich

areas may be qualitatively characterized by the dashed and dot-dashed lines, which denote 10% and 90% photonic fractions, respectively. As the BCS polariton condensate, which is of major interest here, has approximately equal densities of fermionic quasiparticles (n_{eh}) and excitons ($n_{\text{pl-ex}}$), we calculate the difference of these two density fractions by using Figs. 3(a) and 3(b), and show the result in Fig. 1. Masking further the photon-rare and photon-rich areas on it, we then obtain a phase diagram.

We may identify three phases. In the top-left corner of the phase diagram (Fig. 1), photons are basically absent and carriers are dominated by excitons, forming an exciton condensate. On the contrary, in the bottom-right corner of the figure, carriers are mostly photons, giving rise to a photonic polariton condensate, as discussed earlier. In between, it is interesting to see a large phase space for the BCS polariton condensate, with nearly equal numbers of fermionic quasiparticles and excitons, both of which couple to photons. This is the main result of our work. We note that, compared with earlier mean-field predictions [21], we do not find a BCS superfluid with *e-h* pairs only. There, the *e-h* BCS state is indirectly determined from the mean-field pair wave function, which shows a peak in momentum space [21,22]. Our way of comparing the numbers of fermionic quasiparticles and excitons seems to be more direct and reasonable. We also note that, the large phase space of BCS polariton condensate is a consequence of the very strong light-matter coupling. If we decrease the coupling by a factor of 10 (i.e., *strong* light-matter coupling regime), in the low-carrier-density limit we instead observe a conventional exciton-polariton condensate and the window for a BCS polariton condensate becomes considerably narrower [36].

Photonic spectra. How to experimentally probe the intriguing strongly correlated BCS polariton condensate? A unique advantage of an electron-hole-photon system is that its photoluminescence provides direct information of underlying many-body physics. Therefore, we consider the photonic spectral function $\mathcal{A}(\mathbf{q}, \omega) \equiv -(1/\pi)\text{Im}\mathcal{D}(\mathbf{q}, i\nu_n \to \omega + i0^+)$, which experimentally corresponds to the absorption coefficient. Here, the Green's function of photons $\mathcal{D}(\mathcal{Q}) = [\text{diag}\{D_0(\mathcal{Q}), D_0(-\mathcal{Q})\} - \Sigma_{\text{ph}}(\mathcal{Q})]^{-1}$ can be calculated by using the free Green's function $D_0(\mathcal{Q}) = [i\nu_n - \hbar^2\mathbf{q}^2/(2m_{\text{ph}}) + \mu_{\text{ph}} - \delta + g^2/u]^{-1}$ and the photon self-energy

$$\Sigma_{\text{ph}}(\mathcal{Q}) = \frac{g^2}{u^2}\begin{bmatrix} B(\mathcal{Q}) - M_{11} & M_{12} \\ M_{21} & B(-\mathcal{Q}) - M_{22} \end{bmatrix}^{-1}, \quad (8)$$

with $B(\mathcal{Q}) \equiv u^{-1} - u_{\text{eff}}^{-1}(\mathcal{Q})$ [36].

In Fig. 4, we report the absorption coefficient vs momentum and energy at zero detuning $\delta = -E_B$ and at $\Omega = 0.8E_B$, with increasing carrier density from the dilute limit [Fig. 4(a)] to the Mott transition [Fig. 4(d)]. There are always two bright branches, exhibiting an avoided crossing at certain momentum. The lower branch can be identified as the *gapless* Goldstone mode, since the excitation energy ω goes to *zero* as momentum q vanishes [36,43]. It stays within the energy gap for single-particle excitations (i.e., $|\omega| < 2E_{\text{gap}}$, the threshold for two-particle continuum) and therefore should behave like a delta peak if we do not consider any spectral broadening. On the other hand, the upper branch can enter the two-particle
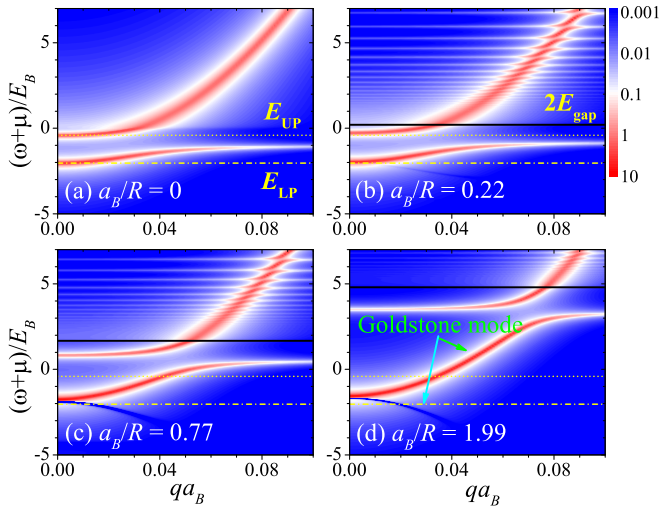
FIG. 4. Absorption coefficient $\mathcal{A}(q, \omega)$ (in arbitrary units and in logarithmic scale) at different inverse mean carrier separations(a) $1/R = 0$, (b) $0.22a_B^{-1}$, (c) $0.77a_B^{-1}$, and (d) $1.99a_B^{-1}$, and at zero detuning $\delta = -E_B$ and the Rabi coupling $\Omega = 0.8E_B$. The wave-vector q is in units of a_B^{-1} and the frequency ω is in units of E_B. The yellow dot-dashed lines and dotted lines show the lower- and upper-polariton energies in the zero-density limit, respectively. The solid black lines is the threshold of two-particle continuum, $E_{\text{th}} = 2E_{\text{gap}}$, where E_{gap} is the energy gap for single-particle excitations. For better illustration, a spectral broadening of $0.05E_B$ is used.
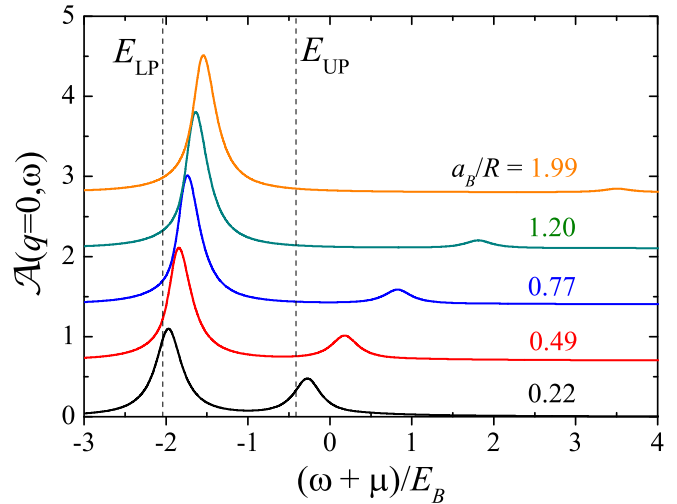

FIG. 5. $\mathcal{A}(\mathbf{q} = 0, \omega)$ (in arbitrary units) at different inverse mean particle distances as indicated. Here, the cavity detuning $\delta = -E_B$ and the Rabi coupling $\Omega = 0.8E_B$. The two dashed lines show the lower-polariton and upper-polariton energies in the zero-density limit. The frequency ω is in units of E_B. We have used a spectral broadening of $0.2E_B$.

continuum. As a result, this branch has an intrinsic spectral width, as indicated by a lot of additional irregular wave-like structures at $\omega > 2E_{\text{gap}}$. In the low-density limit, we may also recognize the two branches as the lower- and upper-polariton branches, respectively. In such a understanding, as the carrier density increases, the upper-polariton energy gets strongly renormalized.

This can be seen more clearly from the carrier density dependence of the spectral function at zero momentum $\mathcal{A}(\mathbf{q} = 0, \omega)$, as shown in Fig. 5. Here, the high-energy peak shows a rapid blueshift with increasing carrier density or with decreasing mean separation R. It is interesting that such a shift is in a qualitative agreement with the recent observation of a high-energy side peak in photoluminescence in high-carrier-density regime, which turns out to be difficult to understand theoretically in terms of Mollow's triplet [11]. We also find that the energy of the lower polaritons shifts up

gradually towards the cavity photon energy $E_{\text{cav}} = -E_B$. This blueshift is well known and has been phenomenologically attributed to the polariton-polariton interaction [1]. Our result provides a useful explanation based on the microscopic model calculation.

Conclusions. We have presented a microscopic, beyond-mean-field study of a strongly interacting exciton-polariton condensate at high density, the so-called BCS polariton condensate. In our theoretical modeling, polariton quasiparticles emerge as quantum fluctuations and their direct characterization allows us to determine the phase diagram with an improved accuracy. We have found that the BCS polariton phase occupies a significant phase space at very strong light-matter coupling. We have predicted the photoluminescence spectra, which might be useful for its eventual experimental confirmation.

[1] H. Deng, H. Haug, and Y. Yamamoto, Exciton-polariton Bose-Einstein condensation, Rev. Mod. Phys. **82**, 1489 (2010).

[2] I. Carusotto and C. Ciuti, Quantum fluids of light, Rev. Mod. Phys. **85**, 299 (2013).

[3] T. Byrnes, N. Y. Kim, and Y. Yamamoto, Exciton-polariton condensates, Nat. Phys. **10**, 803 (2014).

[4] C. Schneider, K. Winkler, M. D. Fraser, M. Kamp, Y. Yamamoto, E. A. Ostrovskaya, and S. Höfling, Exciton-

polariton trapping and potential landscape engineering, Rep. Prog. Phys. **80**, 016503 (2017).

[5] M. D. Fraser, S. Höfling, and Y. Yamamoto, Physics and applications of exciton-polariton lasers, Nat. Mater. **15**, 1049 (2016).

[6] D. Sanvitto and S. Kéna-Cohen, The road towards polaritonic devices, Nat. Mater. **15**, 1061 (2016).

[7] J. Keeling, F. M. Marchetti, M. H. Szymańska, and P. B. Littlewood, Collective coherence in planar semi-

conductor microcavities, Semicond. Sci. Technol. **22**, R1 (2007).

[8] Y. Ohashi and A. Griffin, BCS-BEC Crossover in a Gas of Fermi Atoms with a Feshbach Resonance, Phys. Rev. Lett. **89**, 130402 (2002).

[9] D. S. Citrin and J. B. Khurgin, Microcavity effect on the electron-hole relative motion in semiconductor quantum wells, Phys. Rev. B **68**, 205325 (2003).

[10] X.-J. Liu and H. Hu, Self-consistent theory of atomic Fermi gases with a Feshbach resonance at the superfluid transition, Phys. Rev. A **72**, 063613 (2005).

[11] T. Horikiri, M. Yamaguchi, K. Kamide, Y. Matsuo, T. Byrnes, N. Ishida, A. Löffler, S. Höfling, Y. Shikano, T. Ogawa, A. Forchel, and Y. Yamamoto, High-energy side-peak emission of exciton-polariton condensates in high density regime, Sci. Rep. **6**, 25655 (2016).

[12] T. Horikiri, T. Byrnes, K. Kusudo, N. Ishida, Y. Matsuo, Y. Shikano, A. Löffler, S. Höfling, A. Forchel, and Y. Yamamoto, Highly excited exciton-polariton condensates, Phys. Rev. B **95**, 245122 (2017).

[13] E. Estrecho, T. Gao, N. Bobrovska, D. Comber-Todd, M. D. Fraser, M. Steger, K. West, L. N. Pfeiffer, J. Levinsen, M. M. Parish, T. C. H. Liew, M. Matuszewski, D. W. Snoke, A. G. Truscott, and E. A. Ostrovskaya, Direct measurement of polariton-polariton interaction strength in the Thomas-Fermi regime of exciton-polariton condensation, Phys. Rev. B **100**, 035306 (2019).

[14] J. Hu, Z. Wang, S. Kim, H. Deng, S. Brodbeck, C. Schneider, S. Höfling, N. H. Kwong, and R. Binder, Signature of a Bardeen-Cooper-Schrieffer polariton laser, arXiv:1902.00142v1.

[15] S. Brodbeck, S. De Liberato, M. Amthor, M. Klaas, M. Kamp, L. Worschech, C. Schneider, and S. Höfling, Experimental Verification of the Very Strong Coupling Regime in a GaAs Quantum Well Microcavity, Phys. Rev. Lett. **119**, 027401 (2017).

[16] A. F. Kockum, A. Miranowicz, S. D. Liberato, S. Savasta, and F. Nori, Ultrastrong coupling between light and matter, Nat. Rev. Phys. **1**, 19 (2019).

[17] V. M. Loktev, R. M. Quick, and S. G. Sharapov, Phase fluctuations and pseudogap phenomena, Phys. Rep. **349**, 1 (2001).

[18] P. R. Eastham and P. B. Littlewood, Bose condensation of cavity polaritons beyond the linear regime: The thermal equilibrium of a model microcavity, Phys. Rev. B **64**, 235101 (2001).

[19] J. Keeling, P. R. Eastham, M. H. Szymańska, and P. B. Littlewood, Polariton Condensation with Localized Excitons and Propagating Photons, Phys. Rev. Lett. **93**, 226403 (2004).

[20] J. Keeling, P. R. Eastham, M. H. Szymańska, and P. B. Littlewood, BCS-BEC crossover in a system of microcavity polaritons, Phys. Rev. B **72**, 115320 (2005).

[21] K. Kamide and T. Ogawa, What Determines the Wave Function of Electron-Hole Pairs in Polariton Condensates? Phys. Rev. Lett. **105**, 056401 (2010).

[22] T. Byrnes, T. Horikiri, N. Ishida, and Y. Yamamoto, BCS Wave-Function Approach to the BEC-BCS Crossover of Exciton-Polariton Condensates, Phys. Rev. Lett. **105**, 186402 (2010).

[23] F. Xue, F. Wu, M. Xie, J.-J. Su, and A. H. MacDonald, Microscopic theory of equilibrium polariton condensates, Phys. Rev. B **94**, 235302 (2016).

[24] V. Makhalov, K. Martiyanov, and A. Turlapov, Ground-State Pressure of Quasi-2D Fermi and Bose Gases, Phys. Rev. Lett. **112**, 045301 (2014).

[25] L. He, H. Lü, G. Cao, H. Hu, and X.-J. Liu, Quantum fluctuations in the BCS-BEC crossover of two-dimensional Fermi gases, Phys. Rev. A **92**, 023620 (2015).

[26] Y. Ohashi and A. Griffin, Superfluidity and collective modes in a uniform gas of Fermi atoms with a Feshbach resonance, Phys. Rev. A **67**, 063612 (2003).

[27] H. Hu, X.-J. Liu, and P. D. Drummond, Equation of state of a superfluid Fermi gas in the BCS-BEC crossover, Europhys. Lett. **74**, 574 (2006).

[28] H. Hu, P. D. Drummond, and X.-J. Liu, Universal thermodynamics of strongly interacting Fermi gases, Nat. Phys. **3**, 469 (2007).

[29] R. B. Diener, R. Sensarma, and M. Randeria, Quantum fluctuations in the superfluid state of the BCS-BEC crossover, Phys. Rev. A **77**, 023626 (2008).

[30] M. Yamaguchi, K. Kamide, T. Ogawa, and Y. Yamamoto, BEC–BCS-laser crossover in Coulomb-correlated electron–hole–photon systems, New J. Phys. **14**, 065001 (2012).

[31] Y. Sun, P. Wen, Y. Yoon, G. Liu, M. Steger, L. N. Pfeiffer, K. West, D. W. Snoke, and K. A. Nelson, Bose-Einstein Condensation of Long-Lifetime Polaritons in Thermal Equilibrium, Phys. Rev. Lett. **118**, 016602 (2017).

[32] M. Yamaguchi, K. Kamide, R. Nii, T. Ogawa, and Y. Yamamoto, Second Thresholds in BEC-BCS-Laser Crossover of Exciton-Polariton Systems, Phys. Rev. Lett. **111**, 026404 (2013).

[33] M. Yamaguchi, R. Nii, K. Kamide, T. Ogawa, and Y. Yamamoto, Generating functional approach for spontaneous coherence in semiconductor electron-hole-photon systems, Phys. Rev. B **91**, 115129 (2015).

[34] R. Hanai, P. B. Littlewood, and Y. Ohashi, Photoluminescence and gain/absorption spectra of a driven-dissipative electron-hole-photon condensate, Phys. Rev. B **97**, 245302 (2018).

[35] N. Ishida, T. Byrnes, T. Horikiri, F. Nori, and Y. Yamamoto, Photoluminescence of high-density exciton-polariton condensates, Phys. Rev. B **90**, 241304(R) (2014).

[36] See Supplemental Material at http://link.aps.org/supplemental/10.1103/PhysRevA.101.011602 for the discussions on the two-body physics, the renormalization of the parameters (u_0, g_0, and δ_0), the many-body Gaussian pair fluctuation theory, the carrier density dependence of the chemical potential, the emergent bosons in a two-dimensional Fermi gas at the BEC-BCS crossover, and the phase diagrams at strong light-matter coupling.

[37] E. L. Hazlett, Y. Zhang, R. W. Stites, and K. M. O' Hara, Realization of a Resonant Fermi Gas with a Large Effective Range, Phys. Rev. Lett. **108**, 045304 (2012).

[38] H. Hu, B. C. Mulkerin, U. Toniolo, L. He, and X.-J. Liu, Reduced Quantum Anomaly in a Quasi-Two-Dimensional Fermi Superfluid: Significance of the Confinement-Induced Effective Range of Interactions, Phys. Rev. Lett. **122**, 070401 (2019).

[39] F. Wu, J. Hu, L. He, X.-J. Liu, and H. Hu, Effective theory for ultracold strongly interacting fermionic atoms in two dimensions, arXiv:1906.08578v1.

[40] In the seminal work by Yoji Ohashi and Allan Griffin [26], the number equation for carriers in the GPF theory is written in

terms of Green's functions, which may not be appropriate in the strongly interacting regime due to the truncation at different levels of approximation, as first pointed out by Keeling *et al.* [20]. This possible weakness was later removed by the present authors [27] and Denier *et al.* [29].

[41] In the normal state ($\Delta = 0$), the expression for fermionic quasiparticles reduces to $n_{\text{eh}} = \sum_{\mathbf{k}} 1/[1 + e^{\xi_{\mathbf{k}}/(k_B T)}]$, which is the half of the density of a non-interacting Fermi gas of electrons and holes. In the superfluid phase, we may naively identify n_{eh} as the number of weakly bound, strongly overlapping *e-h* pairs.

This interpretation is not accurate in the BCS limit, where the number of *e-h* pairs goes to zero.

[42] J. Levinsen, G. Li, and M. M. Parish, Microscopic description of exciton-polaritons in microcavities, Phys. Rev. Res. **1**, 033120 (2019).

[43] This may not be so obvious in Fig. 4. We note that, in our calculations the excitation energy ω in the photonic spectral function $\mathcal{A}(\mathbf{q}, \omega)$ is measured from the chemical potential μ. To show the excitation energy as observed in the experiments, we need to plot $\mathcal{A}(\mathbf{q}, \omega)$ as a function of $\omega + \mu$.